Spectral properties of photonic crystal double heterostructure resonant cavities

Adam Mock, Ling Lu and J. D. O'Brien

Department of Electrical Engineering-Electrophysics, University of Southern California
Biegler Hall of Engineering, 920 Downey Way, Los Angeles CA 90089, USA

amock@usc.edu

Abstract: Spectral properties of photonic crystal double heterostructure resonant cavities are calculated numerically using the three-dimensional finite-difference time-domain method. Resonance frequencies and quality factors are reported for various bound states that form near stationary points in the photonic crystal dispersion diagram. The associated electric field spatial profiles are presented indicating potential for in-plane laser optimization. In addition, Fabry-Perot oscillations are observed in the spectra.

OCIS codes: (130.3120) Integrated optics devices; (140.3410) Laser resonators.

References and links

1. C. Zhang, F. Qiao, J. Wan and J. Zi, "Large frequency range of neglible transmission in one-dimensional photonic quantum well structures," Appl. Phys. Lett. **73,** 2084 (1998).
2. N. Stefanou, V. Yannopapas and A. Modinos, "Heterostructures of photonic crystals: frequency bands and transmission coefficients," Comput. Phys. Commum. **113,** 39 (1998).
3. C. Zhang, F. Qiao, J. Wan and J. Zi, "Enlargement of nontransmission frequency range in photonic crystals by using multiple heterostructures," J. Appl. Phys. **87,** 3174 (2000).
4. E. Istrate, M. Charbonneau-Lefort and E. H. Sargent, "Theory of photonic crystal heterostructures," Phys. Rev. B **66,** 075121 (2002).
5. B.-S. Song, T. Asano, and S. Noda, "Heterostructures in two-dimensional photonic-crystal slabs and their application to nanocavities," J. Phys. D **40,** 2629–2634 (2007).
6. Y. Takahashi, H. Hagino, Y. Tanaka, B.-S. Song, T. Asano and S. Noda, "High-Q nanocavity with a 2-ns photon lifetime," Opt. Express **15** 17206–17213 (2007).
7. S. Noda, M. Fujita and T. Asano, "Spontaneous-emission control by photonic crystals and nanocavities," Nat. Photonics **1,** 449–458 (2007).
8. E. Istrate and E.H. Sargent, "Photonic crystal heterostructures and interfaces," Rev. Mod. Phy. **78,** 455–481 (2006).
9. E. Istrate and E. H. Sargent, "Photonic crystal heterostructures–resonant tunnelling, waveguides and filters," J. Opt. A, **4,** S242–S246 (2 002).
10. A. Sharkawy, S. Shi and D. W. Prather, "Heterostructure Photonic Crystals: Theory and Applications," Appl. Opt. **41,** 7245–7253 (2002).
11. E. Kuramochi, M. Notomi, S. Mitsugi, A. Shinya and T. Tanabe, "Ultrahigh-Q photonic crystal nanocavities realized by the local width modulation of a line defect," Appl. Phys. Lett. **88,** 041112 (2006).
12. S. Tomljenovic-Hanic, C. M. de Sterke and M. J. Steel, "Design of high-Q cavities in photonic crystal slab heterostructures by air-holes infiltration," Opt. Express **14** 12451–12456 (2006).
13. C. L. C. Smith, D. K. C. Wu, M. W. Lee, C. Monat, S. Tomljenovic-Hanic, C. Grillet, B. J. Eggleton, D. Freeman, Y. Ruan, S. Madden, B. Luther-Davies, H. Giessen, Y.-H. Lee, "Microfluidic photonic crystal double heterostructures," Appl. Phys. Lett. **91,** 121103 (2007).
14. S. Tomljenovic-Hanic, M. J. Steel, C. M. de Sterke and D. J. Moss, "High-Q cavities in photosensitive photonic crystals," Opt. Lett. **32,** 542–544 (2007).
15. S.-H. Kwon, T. Sunner, M. Kamp and A. Forchel,"Ultrahigh-Q photonic crystal cavity created by modulating air hole radius of a waveguide," Opt. Express **16,** 4605 (2008).
16. L. Lu, T. Yang, A. Mock, M. H. Shih, E. H. Hwang, M. Bagheri, A. Stapleton, S. Farrell, J. D. OBrien and P. D. Dapkus, "100 μW Edge-Emitting Peak Power from a Photonic Crystal Double-Heterostructure Laser," in *Conference on Laser and Electro-Optics* Technical Digest, (2007) paper CMV3.

#94517 - $15.00 USD Received 1 Apr 2008; revised 7 May 2008; accepted 30 May 2008; published 11 Jun 2008

17. T. Yang, S. Lipson, A. Mock, J. D. O'Brien and D. G. Deppe, "Edge-emitting photonic crystal double-heterostructure nanocavity lasers with InAs quantum dot active material," Opt. Lett. **32,** 1153–1155 (2007).
18. M. H. Shih, W. Kuang, A. Mock, M. Bagheri, E. H. Hwang, J. D. O'Brien and P. D. Dapkus, "High-quality-factor photonic crystal heterostructure laser," Appl. Phys. Lett. **89,** 101104 (2006).
19. B.-S. Song, S. Noda, T. Asano and Y. Akahane, "Ultra-high-Q photonic double-heterostructure nanocavity," Nat. Mater. **4,** 207–210 (2005).
20. S. Dey and R. Mittra, "Efficient computation of resonant frequencies and quality factors of cavities via a combination of the finite-difference time-domain technique and the Pade approximation," IEEE Microwave Guid. Wave Lett. **8,** 415–417 (1998).
21. M. H. Shih, W. Kuang, T. Yang, M. Bagheri, Z.-J. Wei, S.-J. Choi, L. Lu, J. D. O'Brien and P. D. Dapkus, "Experimental characterization of the optical loss of sapphire-bonded photonic crystal laser cavities," IEEE Photon. Technol. Lett. **18** 535–537 (2006).
22. O. Painter, R. K. Lee, A. Scherer, A. Yariv, J. D. O'Brien, P. D. Dapkus and I. Kim "Two-dimensional photonic band-gap defect mode laser," Science **284** 1819–1821 (1999).
23. A. Oppenheim and R. Schafer, *Discrete-Time Signal Processing* (Prentice Hall, Upper Saddle River, NJ, 1999).
24. B.-S. Song, T. Asano, Y. Akahane, Y. Tanaka and S. Noda, "Transmission and reflection characteristics of in-plane hetero-photonic crystals," Appl. Phys. Lett. **85,** 4591–4593 (2004).

1. Introduction

Both passive and active materials in planar slab geometries patterned with two-dimensional photonic crystals are interesting candidates for optical integrated circuits due to their flexibility and small size. The theoretical properties of photonic crystal heterostructures have been investigated over the last several years [1, 2, 3, 4]. The photonic crystal double heterostructure (PCDH) pictured in Fig. 1(b) has recently been shown to have an experimental cold cavity quality factor (Q) of over 10^6 and a mode volume on the order of a cubic optical wavelength [5, 6, 7] making this geometry a good candidate for compact chip-scale sources and filters [8, 9, 10]. Other methods of forming PCDH cavities have been reported including local modulation of a photonic crystal line defect width [11], local air-hole infiltration [12, 13], local change in membrane refractive index in photosensitive materials [14] and local modulation of the hole radii [15].

In addition, the waveguide-like shape of these cavities enhances their edge-emission and ability to channel electromagnetic energy directly into adjoining photonic crystal waveguides (PCWG) [16, 17]. PCDH cavities may also be formed by locally decreasing the lattice constant as shown in Fig. 1(c). Furthermore, one may perturb the lattice in two-dimensions, and experimental lasing results for this type of perturbation have been reported [18]. In this work, we extend the theoretical understanding of the PCDH with a detailed analysis of PCDH cavity spectra that indicates the presence of bound states near stationary points in the PCWG dispersion diagram associated with the unperturbed sections of the PCDH. With this information one can use PCWG dispersion diagrams to predict resonance frequencies and understand other features of numerical and experimental resonance spectra. Furthermore, we present mode profiles for several bound state resonances whose in plane confinment properties differ significantly. This added information is useful in designing PCDH lasers for edge emission.

2. 3-D FDTD Analysis of photonic crystal double heterostructure resonant cavities

Figure 1(a) shows a single line defect PCWG dispersion diagram calculated using the three-dimensional finite-difference time-domain (FDTD) algorithm. The index of refraction of the slab is 3.4, its thickness is $0.6a$ and the hole radii are $0.3a$ where a is the period of the photonic crystal hole spacing. Because Bloch boundary conditions are implemented along the propagation direction, only a single unit cell of the PCWG is stored in memory, and the computational resources required are moderate. In the case of PCDH cavities, the computational resources required are significant, as the number of PCWG cladding periods on either side of the defect area must be enough to simulate an effectively infinitely long waveguide. Adjacent to the PCWG bandstructure in Fig. 1(a) are resonance spectra of two PCDH: one for a positive defect and one

#94517 - $15.00 USD Received 1 Apr 2008; revised 7 May 2008; accepted 30 May 2008; published 11 Jun 2008

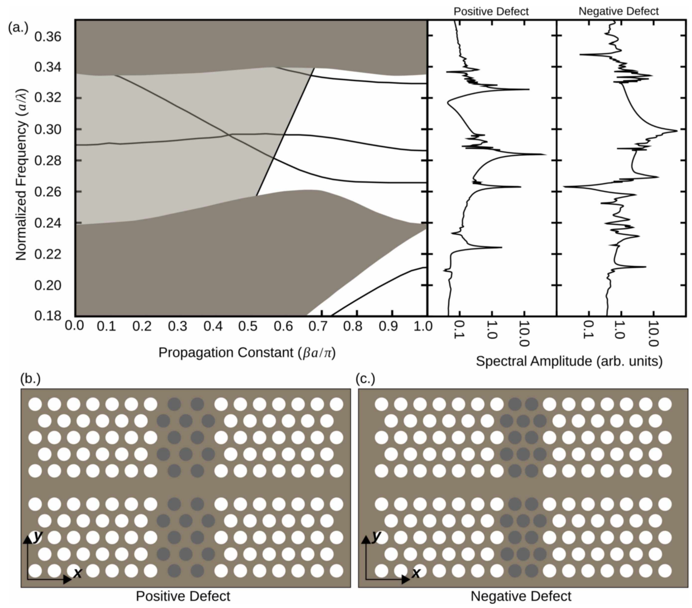

Fig. 1. (a.) Left: Single line defect air-clad photonic crystal waveguide dispersion diagram. Dark gray indicates photonic crystal cladding modes. Light gray indicates slab radiation modes. Right: Photonic crystal double-heterostructure (PCDH) resonance spectra for positive and negative defects. (b.) Top view of PCDH with one-dimensional positive defect. (c.) Top view of PCDH with one-dimentional negative defect. Darkened circles are perturbed.

for a negative defect. The material properties are the same as for the PCWG calculation, and the lattice constant perturbation is +5% for the positive defect and -5% for the negative defect. We are working with a 5% perturbation here as opposed to the 2.5% perturbations reported by [5] to separate the bound state resonance from the PCWG Fabry-Perot resonances which will be discussed in Section 4. This increased spectral separation made obtaining mode profiles through spectral filtering and the numerical estimation of Q more reliable. Increasing the perturbation tends to lower the Q of these devices; however, this difference does not effect the conclusions regarding the general PCDH concepts made in this work.

The perturbation is along x only, and there are 20 PCWG periods on either side of the defect. These spectra were obtained by taking a discrete Fourier transform of a 200000 time-step sequence initialized with a broad-band source. The time-step sequences required about 20 hours of computation on 100 parallelized processors.

3. Properties of photonic crystal double heterostructure bound states

In the PCWG dispersion diagram, there are three waveguide modes in the photonic crystal bandgap with one additional mode just below the photonic crystal cladding modes. These modes have TE-like symmetry, and the corresponding bandgap is the lowest frequency bandgap with TE-like symmetry. Increasing (decreasing) the lattice constant of a few periods of the otherwise uniform PCWG shifts the local bandstructure at the perturbation down (up). In comparing the two spectra to the PCWG dispersion in Fig. 1(a), one can see that there are resonance peaks near stationary points in the unperturbed waveguide dispersion. When the lattice constant is locally increased (decreased), the bound state forms near stationary points that are concave up (down). Only below and above (for positive and negative defects, respectively) the extrema of the dispersion relation in the uniform PCWG regions is there a possibility for a mode to exist in

#94517 - $15.00 USD Received 1 Apr 2008; revised 7 May 2008; accepted 30 May 2008; published 11 Jun 2008

the central region without the possibility of there simultaneously being a mode in the cladding at the same frequency a small distance in wave vector away. In other words, only in these cases is there no mode that is nearby (in the wavevector sense) in the cladding at the same frequency. This mode formation is analogous to the formation of bound states in electronic heterostructures at the extrema of the electronic dispersion relations.

Table 1. Resonance frequencies and quality factors for a PCDH with $\Delta a = 5\%$ in one dimension. Frequencies are in normalized units (a/λ). Spectral resolution is 0.0002.

Resonance Frequency	PCWG Stationary PointFrequency	Quality Factor	Perturbation
0.2115	0.2112	1130	-
0.2628	0.2654	266000	+
0.2837	0.2861	12700	+
0.2986	0.2968	260	-
0.3252	0.3290	8820	+

Table 2. Resonance frequencies and quality factors for a PCDH with $\Delta a = 5\%$ in two dimensions. Frequencies are in normalized units (a/λ). Spectral resolution is 0.0002.

Resonance Frequency	PCWG Stationary Point Frequency	Quality Factor	Perturbation
0.2116	0.2112	1190	-
0.2621	0.2654	141000	+
0.2835	0.2861	2230	+
0.3002	0.2968	238	-
0.3217	0.3290	1930	+

The quality factors of the different bound states in these PCDH resonant cavities are obtained from the resonance spectra by dividing the resonance frequency, f_0, by the full width at half maximum (FWHM), Δf, or $Q = f_0/\Delta f$. Our simulation technique consists of a spatially random distribution of broad band initial conditions. The resonant modes are excited, and the energy gradually leaks out of the cavity upon subsequent time stepping. The characteristic ring-down time of the different modes gives rise to the corresponding spectral width. Error due to early truncation of the time sequence is reduced using the Padé interpolation method [20]. Center frequencies and Qs for bound states formed in PCDH cavities with defects formed by increasing (+) or decreasing (-) the lattice constant by 5% in one-dimension are summarized in Table 1. The corresponding results for a two-dimensional perturbation are shown in Table 2. As discussed previously, the bound state frequencies are just below (above) the PCWG band edge for PCDH cavities formed by positive (negative) defects.

The high quality factor of the second mode listed in Table 1 has been discussed by [5, 19]. However, pointing out that PCDH bound states form near any stationary point in the dispersion diagram with varying quality factors is useful for semiconductor laser applications. To achive laser operation, only moderate quality factors having values around 1000 are required [16, 21] with the first demonstration of a photonic crystal laser having an estimated passive Q of 250 [22]. Therefore, any of the resonance modes listed in Tables 1 and 2 is a viable candidate for a laser. We attribute the exceptionally low Q of the fourth mode to significant out of plane radiation due to the close proximity to the light line of the concave down stationary point associated

#94517 - $15.00 USD Received 1 Apr 2008; revised 7 May 2008; accepted 30 May 2008; published 11 Jun 2008

with this mode.

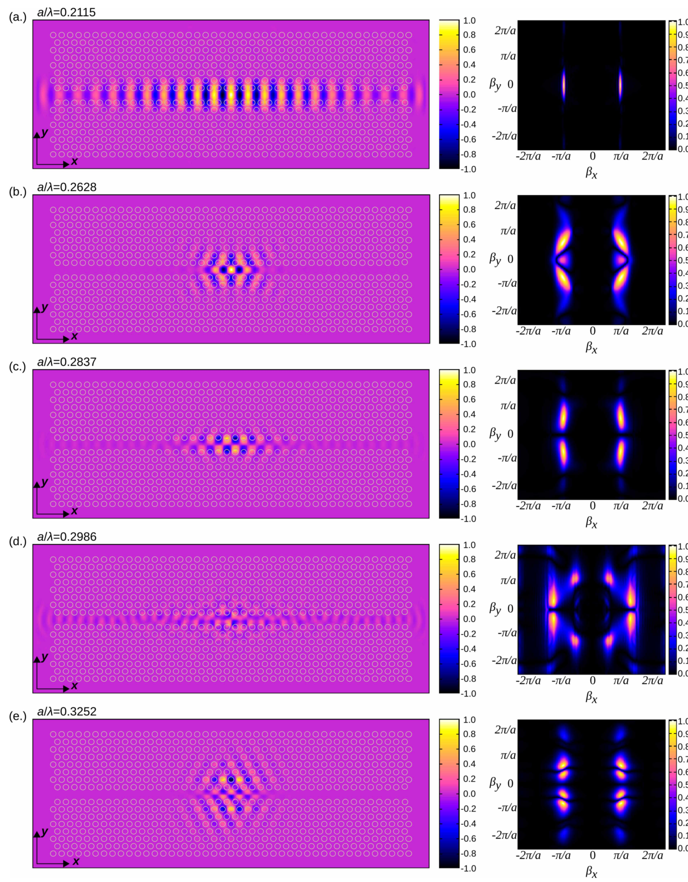

Fig. 2. y-component of the electric field along with their spatial Fourier transforms $E_y(\beta_x,\beta_y)$ for the modes in Table 1.

Spatial mode profiles associated with the different resonances of a PCDH with a one-dimensional defect were obtained from subsequent FDTD runs with a discrete-time filter [23] to isolate the mode of interest. The y-component of the electric field at the midplane of the slab for the bound states associated with each mode in Table 1 is shown in Fig. 2. The mode profiles appear to be approximately uniform PCWG mode profiles multiplied by a confining envelope function centered at the defect. The spatial mode profiles are qualitatively similar for the two-dimensional perturbation.

The qualitative features of the spatial distribution of the $E_y(x,y)$ components are useful in design considerations. To enhance edge-emission along the PCWG direction, a more extended mode such as that shown in Fig. 2(a) would be preferred. For vertical emission and smaller mode volume, the modes in Fig. 2(b) or (c) are the best candidates. Finally, for emission through the photonic crystal cladding, the mode shown in Fig. 2(e) is promising.

Performing a two-dimensional spatial Fourier transform of the field profile at the midplane of the slab reveals the spatial Fourier components that make up the bound state. To the right of each $E_y(x,y)$ spatial mode profile in Fig. 2, spatial Fourier transforms $E_y(\beta_x,\beta_y)$ are shown. All but the mode at $a/\lambda = 0.2986$ have significant spatial Fourier components near the Brillouin zone boundary at $\beta = \pm\frac{\pi}{a}$. The mode at $a/\lambda = 0.2986$ has Fourier components near $\beta_x = \pm 0.6 \times \frac{\pi}{a}$

#94517 - $15.00 USD Received 1 Apr 2008; revised 7 May 2008; accepted 30 May 2008; published 11 Jun 2008

as well as significant amplitude in the second Brillouin zone at $\beta_x = 0.6 \times \frac{\pi}{a} - \frac{2\pi}{a}$ and $\beta_x = -0.6 \times \frac{\pi}{a} + \frac{2\pi}{a}$. All of these results are consistent with the location of the stationary points on the PCWG dispersion diagram: the four bands flatten at $\beta_x = \pm\frac{\pi}{a}$, and the third band peaks at $\beta_x = \pm 0.6 \times \frac{\pi}{a}$.

4. Fabry-Perot resonances

To investigate additional peaks in the resonance spectra near the bound state resonances, PCDH cavities with 40 PCWG cladding periods were analyzed with the idea that these peaks came from Fabry-Perot resonances in the uniform PCWG regions. Figures 3(a) and 3(b) show the resulting spectra.

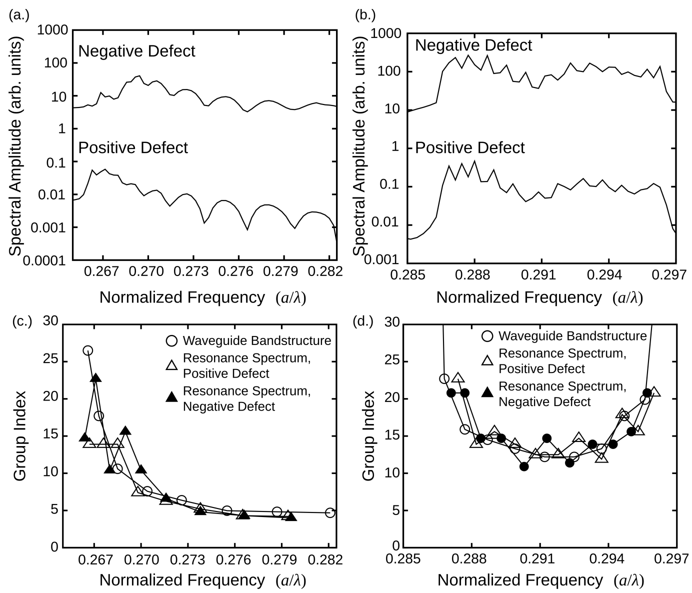

Fig. 3. Spectra for positive and negative defect photonic crystal double-heterostructure (PCDH) cavities for points off center along x for (a.) the second PCWG band and (b.) the third PCWG band. Group index for positive and negative defect (PCDH) cavities along with group index calculated from the photonic crystal waveguide (PCWG) dispersion diagram for (c.) the second PCWG band and (d.) the third PCWG band.

The time sequence is measured a few periods along x from the center of the cavity. Additional resonance peaks in the frequency ranges 0.265-0.285 and 0.285-0.297 are apparent and are present in PCDH cavities with both positive and negative defects. The termination of the uniform PCWG and the interface between the uniform PCWG and the perturbed region form mirrors between which oscillation can occur with a group velocity determined by the slope of the PCWG dispersion diagram [24]. The result of measuring the peak spacing in the PCDH resonance spectra and calculating the corresponding frequency dependent group index according to $n_g = c/2L\Delta f$ where L is the length of one side of the uniform PCWG region is shown in Fig. 3(c) and Fig. 3(d). The agreement between the PCDH peak spacing and PCWG dispersion slope is quite good. We attribute the slight scatter in the data to the low frequency resolution of 0.0003 in normalized frequency.

#94517 - $15.00 USD Received 1 Apr 2008; revised 7 May 2008; accepted 30 May 2008; published 11 Jun 2008

5. Conclusion

In this work we have shown that PCDH bound states form near stationary points in the PCWG dispersion diagram. The bound states form near local minima for positive lattice constant pertubations and near local maxima for negative lattice constant perturbations. Additional Fabry-Perot resonances are observed whose spectral spacing is consistent with the group index dispersion of the the different PCWG bands. This information is useful in predicting and understanding the properties of numerical and experimental PCDH resonance spectra. Because quality factor values around 1000 are sufficient to achieve laser operation in quantum well active regions, several of the bound states described in this paper are candidates for PCDH lasers. The differing confinement properties of the electric field profiles offer a method to optimize cavity geometry for different applications.

Acknowledgments

This study is based on research supported by the Defense Advanced Research Projects Agency (DARPA) under contract No. F49620-02-1-0403 and by the National Science Foundation under grant ECS-0507270. Computation for the work described in this study was supported, in part, by the University of Southern California Center for High Performance Computing and Communications.